Ceramics International 42 (2016) 10066–10070

Contents lists available at ScienceDirect

Ceramics International

journal homepage: www.elsevier.com/locate/ceramint

Effect of gallium doping on the structural, optical and electrical properties of zinc oxide thin films prepared by spray pyrolysis

E. Muchuweni *, T.S. Sathiaraj, H. Nyakotyo

Department of Physics and Astronomy, Botswana International University of Science and Technology (BIUST), P. Bag 16, Palapye, Botswana

ARTICLE INFO

Article history:
Received 26 January 2016
Received in revised form
7 March 2016
Accepted 15 March 2016
Available online 16 March 2016

Keywords:
A. GZO thin films
C. Electrical properties
C. Optical properties
Spray pyrolysis

ABSTRACT

Gallium-doped zinc oxide (GZO) thin films were deposited onto glass substrates by the spray pyrolysis technique and the effect of gallium (Ga) doping on their structural, optical and electrical properties was investigated by X-ray Diffraction (XRD), Spectrophotometry and Current–Voltage (*I–V*) measurements, respectively. XRD studies revealed that all films were polycrystalline in nature, with a hexagonal wurtzite crystal structure and a predominant (002) *c*-axis orientation. Ga doping resulted in deterioration of the film's crystallinity, increase in full width at half maximum (FWHM) and reduction in the mean crystallite sizes. All GZO thin films had relatively higher average transmittances, approximately 70–85% in the visible region as compared to the undoped ZnO thin films. Introduction of Ga led to a blue shift in the optical band gap from 3.26 eV to 3.30 eV and an increase in the Urbach energy from around 67 meV to 100 meV. Ga doping induced a decrease in sheet resistance leading to a minimum electrical resistivity of 1.2 Ω cm and a maximum figure of merit of $1.02 \times 10^{-4}\ \Omega^{-1}$ for the 1 at% GZO thin film, indicating its suitability for optoelectronic applications, especially transparent electrode fabrication.

1. Introduction

In the past few years, there has been much research interest on transparent conducting oxide (TCO) thin films due to their wide use as transparent electrodes in flat screen displays [1], photovoltaic devices [2], light emitting diodes [3] and heat mirrors [4]. The most commonly used TCO material is indium tin oxide (ITO), due to its excellent optical and electrical properties [5,6]. However, due to indium's scarcity, high processing cost and toxicity, there has been much emphasis on finding suitable alternatives [7].

ZnO is a promising alternative material to ITO due to its competitive optical and electrical properties [8,9], low deposition temperature, high chemical and thermal stability [10] combined with zinc's abundance in nature, low cost and non-toxicity [11]. However, undoped ZnO has a relatively low transparency and high resistivity, so it is commonly doped with aluminium (Al) to enhance its electrical and optical properties [12,13]. However, compared to Ga, Al has a relatively poor thermal stability and its high reactivity causes degeneration problems when exposed to ambient air for a long time [14]. Therefore, doping ZnO with Ga is favourable due to its less reactivity and more stability with respect to oxidation [14,15] and its capability of creating a more uniform structure with few lattice defects due to the closer atomic radius of Ga (0.062 nm) to Zn (0.060 nm) than Al (0.052 nm) [8]. Muiva et al. [10], reported that doping plays a significant role in lowering the electrical resistivity through charge carrier multiplication and defect population reduction.

Several synthesis routes, such as spin coating [16], dip coating [17], rf magnetron sputtering [18], electron beam evaporation [19] and spray pyrolysis [20] have been successfully used to deposit GZO thin films. Among these methods, spray pyrolysis has the advantages of safety, simplicity, cheap cost, no high vacuum requirement and well adaptation for large area coatings. To the best of our knowledge, GZO thin films have been relatively less studied than Al doped ZnO thin films [20].

In this work, we report the effect of Ga doping on the structural, optical and electrical properties of GZO thin films prepared on glass substrates by spray pyrolysis. The optimum Ga concentration yielding the best optical and electrical properties is revealed for possible transparent electrode fabrication.

2. Experimental details

GZO thin films were deposited onto glass substrates (Corning NY 14831, USA) of size (75 mm × 25 mm × 1 mm) using the spray pyrolysis technique. A 0.1 M spray solution was prepared by dissolving zinc acetate dihydrate in a mixture of methanol and deionized (DI) water. The ratio of methanol to DI water was maintained at 13:7. To achieve Ga doping, four different

* Corresponding author.
E-mail address: muchuweniedigar1@gmail.com (E. Muchuweni).

http://dx.doi.org/10.1016/j.ceramint.2016.03.110
0272-8842/

concentrations (1, 2, 3 and 5 at%) of Ga nitrate hydrate were added into the spray solution. A few drops of acetic acid were also added to the spray solution to prevent the formation of zinc hydroxide. Just before deposition, the glass substrates were ultrasonically cleaned with acetone, isopropanol and finally with DI water for 10 min in each step. After cleaning, the substrates were dried at room temperature using compressed air.

Thin films were then deposited by spraying the solution onto clean glass substrates placed on a hot plate stove set at 723.15 K. The solution flow rate was maintained at 3 ml/min throughout the coating process and compressed air was used as the carrier gas to atomize the precursor solution through a nozzle held at 25 cm directly above the substrate. After deposition, the samples were left to cool down to room temperature and then taken for characterization.

The thickness of the films was measured using a 2D surface profilometer (Alpha-step D-100, KLA-Tencor, USA). Crystal structure and orientation of the films were examined using an X-ray diffractometer (XRD, D8 Advance, Bruker, Germany) with Cu Kα radiation (λ = 1.5418 Å), in the 2θ scan range from 10° up to 70°. The average grain sizes were evaluated using the Debye–Scherrer equation from broadening of diffraction peaks. Optical transmittance was measured between 300 and 800 nm range of wavelengths using a UV/Vis/NIR spectrophotometer (Lambda-750, Perkin-Elmer, America). The optical band gap and Urbach energy were obtained from transmission spectrum data. The electrical properties were determined from the sheet resistance using the four point probe equipment comprising of a Signatone probe station, an EZ GP-4303 d.c. source and two Keithley 197 digital multimeters for voltage and current measurements.

3. Results and discussion

3.1. Structural properties

Fig. 1 shows XRD patterns of undoped ZnO and GZO thin films of almost similar thicknesses ranging between 350 and 400 nm, prepared on glass substrates at 723.15 K. Weak (100), (002), (101), (210) and (103) diffraction peaks were observed in most samples, except the absence of the (100) peak in undoped ZnO thin films. All films were polycrystalline with a hexagonal wurtzite structure and a strong orientation along the (002) plane, regardless of the amount of Ga doping. This was in agreement with sprayed GZO thin films by Rao and Kumar [21]. Contrary to our findings, Lokhande and Uplane [22] obtained sprayed ZnO thin films with a preferred growth orientation along the (100) plane. The (002) plane's intensity was observed to decrease for films with higher Ga content and Babar et al. [23], attributed this crystallinity deterioration to crystal reorientation effect emanating from incorporation of more Ga atoms. Winer et al. [8], reported that mechanical stresses caused by differences in the ionic radii of the dopant and Zn may be the possible cause of degradation in crystallinity at higher doping concentrations. Reddy et al. [24] observed a relative decrease in the (002) peak intensity for films with smaller thicknesses, so the slight reduction of thickness values in our films may also be responsible for the decrease in intensity. No extra peaks corresponding to neither Zn or Ga nor Ga_2O_3 were observed indicating the absence of secondary phase formation in our films. This shows that Ga managed to substitute Zn and can reasonably reside on zinc site in the hexagonal lattice [25].

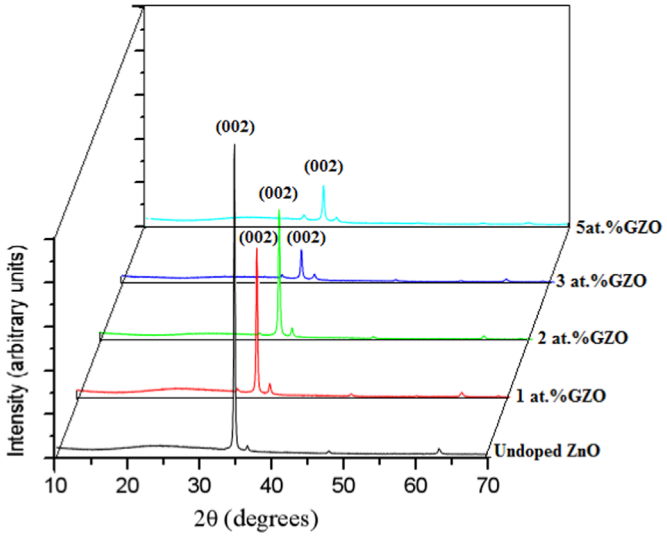

Fig. 1. XRD patterns of undoped ZnO and GZO thin films deposited on glass substrates at 723.15 K.

The mean crystallite size for each sample was calculated according to broadening of the dominant peak corresponding to the (002) diffraction plane using Debye–Scherrer's formula [18]:

$$D = \frac{0.9\lambda}{\beta \cos\theta}, \tag{1}$$

where D, λ, β, and θ are the mean crystallite size, X-ray wavelength (1.5418 Å), FWHM in radians and Bragg's diffraction angle, respectively. The dislocation density δ was also calculated using [26]:

$$\delta = \frac{1}{D^2}, \tag{2}$$

where D is the mean crystallite size. The (002) peak positions, FWHM, mean crystallite sizes and dislocation densities with respect to Ga doping are shown in Table 1.

Ga doping led to the increase in FWHM values and a decrease in the mean grain sizes. From Table 1, it is clear that an increase in Ga content leads to an increase in the dislocation density, which in turn results in the observed reduction of the films' crystallinity qualities. The (002) peak position of GZO thin films showed a slight shift towards a higher Bragg angle relative to that of undoped ZnO thin films. This was may be due to a slight increase in relative strain [23] originating from the substitution of Zn^{2+} ions with relatively smaller Ga^{3+} ions [7].

The lattice parameters a and c were calculated using the equation [27,28]:

$$\frac{1}{d_{hkl}^2} = \frac{4}{3}\left(\frac{h^2 + hk + k^2}{a^2}\right) + \frac{l^2}{c^2}, \tag{3}$$

where d_{hkl} is the interplanar spacing obtained from Bragg's law, and h, k and l are the Miller indices denoting the plane. Ga doping did not produce a significant change in the lattice parameters since the undoped ZnO and all GZO films had approximately equal lattice parameters, a=3.21 Å and c=5.14 Å. These values are slightly less than those for bulk ZnO, a=3.22 Å and c=5.2 Å,

Table 1
The (002) peak position, FWHM, grain size and dislocation density of undoped ZnO and GZO thin films.

GZO (at%)	(002) peak position 2θ (°)	β (°)	D (nm)	δ ($\times 10^{-4}$ nm^{-2})
0	34.899	0.198	42.04	5.66
1	34.899	0.207	40.20	6.19
2	34.917	0.244	34.12	8.59
3	34.917	0.251	33.21	9.07
5	34.899	0.290	28.68	12.16

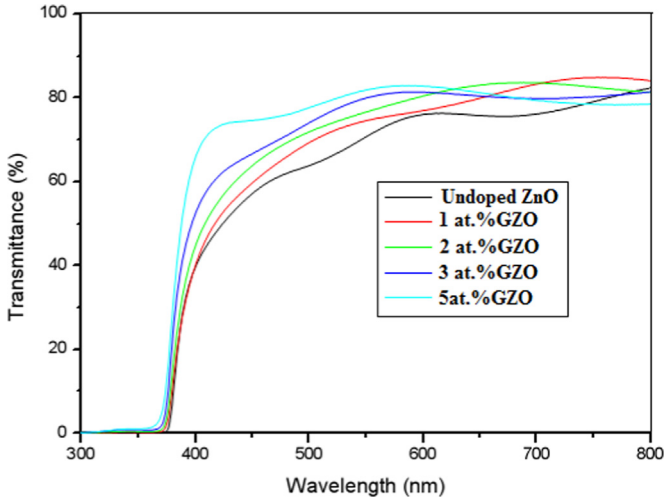

Fig. 2. Optical transmission spectra of the undoped ZnO and GZO thin films.

JCPDS: 36–1451 [29], may be due to very small amounts of compressive strain in the films.

The strain ε and stress σ along the c-axis were calculated using the equations [30,31]:

$$\varepsilon = \frac{c_{film} - c_{bulk}}{c_{bulk}}, \tag{4}$$

$$\sigma = -2.33 \times 10^{11}\left(\frac{c_{film} - c_{bulk}}{c_{bulk}}\right), \tag{5}$$

where c_{film} and c_{bulk} (5.2 Å) are the lattice parameters of the thin film and bulk ZnO, respectively. The undoped ZnO and GZO thin films had equal compressive strains and tensile stresses of -1.15×10^{-2} and 2.69 GPa, respectively. Doping was observed to have insignificant effects on the strain and stress as evidenced by almost similar (002) peak positions and equal lattice parameters for all films.

3.2. Optical properties

Fig. 2 shows the optical transmittance spectrum of undoped ZnO and GZO thin films in the wavelength range from 300 to 800 nm. Interference fringes were observed in the transmission spectrum due to interference of light reflected between the air-film interface and the film-substrate interface. The amplitude of interference fringes decreased for higher doping concentration, indicating a loss in surface smoothness leading to a slight scattering loss [32]. All GZO thin films had relatively higher transparencies (about 70–85%) in the visible region as compared to undoped ZnO thin films. These high transparencies may be attributed to the more porous nature of the GZO thin films. For wavelengths greater than 600 nm, there is a decrease in transparency at higher Ga doping and this may be originating from increased photon scattering by crystal defects created by doping [32]. Sharp absorption edges were observed at approximately 375–380 nm and they blue shifted with the introduction of Ga doping. This observation was in fair agreement with Winer et al. [8] and Rao et al. [21]. This is also consistent with the Burstein–Moss effect [33] and occurs as a result of high charge carrier concentration imposed by higher Ga content [8].

The optical absorption coefficient α was calculated in the high absorption region using the Beer–Lambert law [34]:

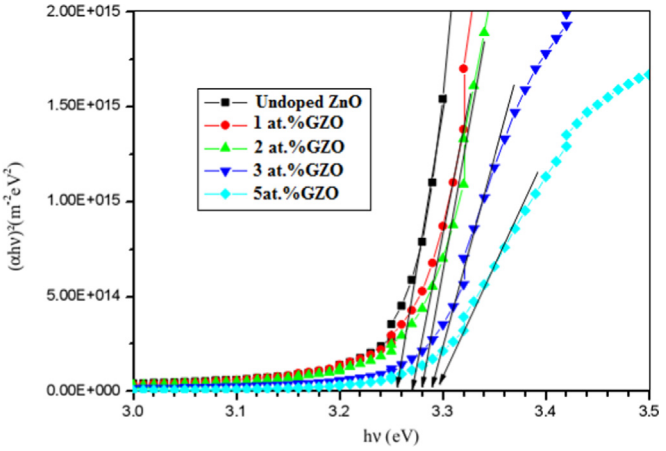

Fig. 3. Variation of $(\alpha h\nu)^2$ versus $(h\nu)$ for the undoped ZnO and GZO thin films.

$$\alpha = \frac{1}{t}\ln\left[\frac{1}{T}\right], \tag{6}$$

where t and T are the film thickness and transmittance, respectively. An estimation of the optical band gap was also made in the high absorption region by assuming a direct transition between the valence band and conduction band, using Tauc's model [35]:

$$(\alpha h\nu)^2 = B(h\nu - E_g), \tag{7}$$

where α is the optical absorption coefficient, $h\nu$ is the energy of the incident photon, B is an energy-independent constant and E_g is optical band gap. E_g values were obtained from Tauc's plot of $(\alpha h\nu)^2$ versus $h\nu$, shown in Fig. 3, by extrapolating the straight line portion of the absorption edge to $(\alpha h\nu) = 0$.

E_g was found to increase from around 3.26 to 3.30 eV with the addition of Ga. This blue shift in E_g values may be attributed to the increase in charge carrier concentration which in turn broadens the energy band [36] in accordance with the Burstein–Moss effect [33]. Zhang et al. [37] attributed the band gap difference between the undoped ZnO thin film and that of the bulk ZnO to grain boundaries, stress and interaction potentials between defects and host materials in the films.

Closer to the absorption band edge, the absorption coefficient exhibits an exponential dependence on photon energy, given by [38]:

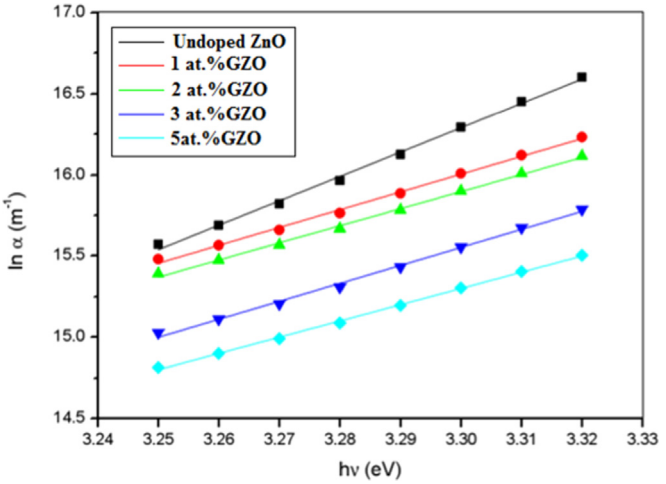

Fig. 4. A plot of $\ln(\alpha)$ versus $h\nu$ of the undoped ZnO and GZO thin films.

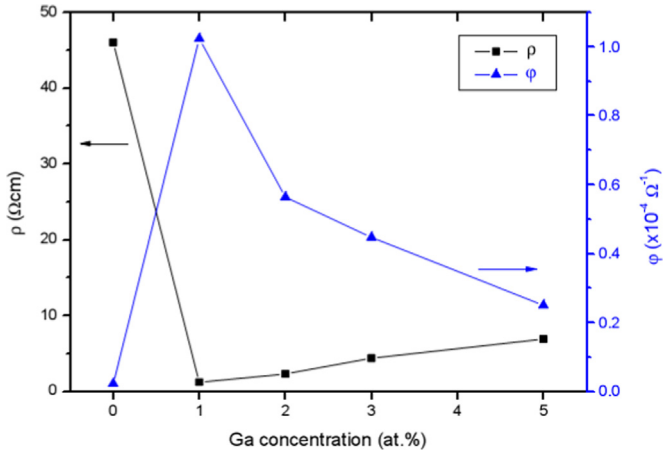

Fig. 5. Variation of the electrical resistivity and figure of merit for GZO thin films deposited at different Ga concentrations.

$$\alpha = \alpha_0 \exp\left(\frac{h\nu}{E_u}\right), \tag{8}$$

where α_0 is a constant and E_u is the Urbach energy obtained from a plot of lnα versus $h\nu$ (Fig. 4).

E_u is interpreted as the width of the tails of localized states in the band gap [39] and is obtained from the reciprocal of the linear portion's gradient (Fig. 4). The value of E_u was observed to increase from around 67 meV to 100 meV with addition of Ga from 0 to 5 at%. This trend was consistent with Rao and Kumar's result [21] and implied that addition of Ga led to an increase in structural disorders and defects as earlier on revealed by XRD analysis.

3.3. Electrical properties

The electrical resistivity ρ of the undoped ZnO and GZO thin films was calculated using the equation [40]:

$$\rho = R_s t, \tag{9}$$

where R_s and t are the sheet resistance and film thickness, respectively. Fig. 5 shows the variation of electrical resistivity of undoped ZnO and GZO thin films as a function of Ga dopant concentration.

From Fig. 5, it was clearly observed that all GZO thin films had lower electrical resistivities as compared to undoped ZnO thin films. The sheet resistivity initially decreased from 46 Ω cm in the undoped ZnO thin film, to its lowest value of 1.2 Ω cm in the 1 at% GZO thin film. This fall in resistivity may be attributed to the rise in free charge carrier concentration as a result of extra electrons being contributed by the donor Ga^{3+} cations incorporated as replacement ions for Zn^{2+} cations [8]. However, a further increase in Ga doping level above 1 at% resulted in an increase in the films' resistivity, may be due to the build up of charge carrier trapping sites at grain boundaries, which lower the carrier mobility in the ZnO lattice [1]. Winer et al. [8] attributed the increase in electrical resistivity at higher Ga doping concentration to crystallinity deterioration emanating from the creation of amorphous non-conducting Ga_2O_3 secondary phase at grain boundaries. Instead of donating charge carriers, the Ga_2O_3 secondary phase traps charge carriers, thus causing an increase in sheet resistivity. However, in this study, no secondary phases were detected in the XRD spectra, so a possible cause for the observed increase in electrical resistivity at higher Ga doping may be degradation in crystallinity and reduction in grain sizes which generate more grain boundaries which in turn reduce carrier mobility.

In a similar study, Winer et al. [8] obtained minimum electrical resistivities in the 1 and 2 at% GZO thin films depending on the precursor solution. Reza et al. [41] also obtained the lowest electrical resistivity in the 1 at% GZO thin film. This was in fair agreement with our findings. However, Rao and Kumar [21] obtained minimum electrical resistivities in the 3 at% GZO thin film. These different values can be attributed to a number of factors including, the use of different deposition parameters and precursor solutions [1,8].

In order to quantify the optoelectronic properties of the prepared GZO thin films for transparent electrode fabrication, the figure of merit (φ) was calculated using the equation [42]:

$$\varphi = \frac{1}{\alpha\rho}, \tag{10}$$

where α is the absorption coefficient at 550 nm and ρ is the electrical resistivity. Babar et al. [23] reported that the highest φ value (the best combination of high transmission and low resistivity) results in TCO films with better quality or performance. Fig. 5 shows φ for GZO thin films as a function of doping concentration. The figure of merit was observed to increase firstly and then decreased with the increment of doping concentration. The best φ ($1.02 \times 10^{-4}\ \Omega^{-1}$) was obtained when the doping concentration was 1 at% and this value is higher than $1.5 \times 10^{-6}\ \Omega^{-1}$ reported for spray deposited ZnO films by Muiva et al. [9]. This indicated that our 1 at% GZO thin films are acceptable candidates in optoelectronic applications such as transparent electrode fabrication.

4. Conclusion

GZO thin films were successfully prepared on glass substrates at 723.15 K using spray pyrolysis and their structural, optical and electrical properties were investigated with respect to Ga doping concentration. XRD studies revealed that all the undoped ZnO and GZO thin films had a polycrystalline hexagonal wurtzite structure with a preferred (002) c-axis orientation. The ZnO thin film's crystallinity was observed to deteriorate with increase in Ga doping concentration. Ga doping also resulted in an increase in the FWHM and dislocation density and a decrease in mean grain sizes. All GZO thin films exhibited relatively higher transparencies (around 70–85%) in the visible region as compared to the undoped ZnO thin film. The optical band gap shifted towards shorter wavelengths with Ga doping, from 3.26 to 3.30 eV, according to the Burstein–Moss effect. There was an observed increase in Urbach energies with Ga addition, indicating the increase in structural disorders and defects, in agreement with XRD analysis. The lowest electrical resistivity (1.2 Ω cm) and highest figure of merit ($1.02 \times 10^{-4}\ \Omega^{-1}$) were obtained in the 1 at% GZO sample implying that such a film can be beneficially used for the fabrication of transparent electrodes.

Acknowledgements

The authors extend their gratitude to Botswana International University of Science and Technology (BIUST) for funding this study.

References

[1] C. Tsay, K. Fan, C. Lei, Synthesis and characterization of sol–gel derived gallium-doped zinc thin films oxide, J. Alloy. Compd. 512 (2012) 216–222.
[2] B. Rech, T. Repmann, S. Wieder, M. Ruske, U. Stephan, A new concept for mass

production of large area thinifilm silicon solar cells on glass, Thin Solid Films 502 (2006) 300–305.
[3] E. Şenadim Tüzemen, H. Kavak, R. Esen, Influence of oxygen pressure of ZnO/glass substrate produced by pulsed filtered cathodic vacuum arc deposition, Phys. B: Condens. Matter 390 (2007) 366–372.
[4] W.J. Jeong, S.K. Kim, G.C. Park, Preparation and characteristic of ZnO thin film with high and low resistivity for an application of solar cell, Thin Solid Films 506 (2006) 180–183.
[5] T.S. Sathiaraj, Effect of annealing on the structural, optical and electrical properties of ITO films by RF sputtering under low vacuum level, Microelectron. J. 39 (2008) 1444–1451.
[6] S. Calnan, H.M. Upadhyaya, M.J. Thwaites, A.N. Tiwari, Properties of indium tin oxide films deposited using high target utilisation sputtering, Thin Solid Films 515 (2007) 6045–6050.
[7] A. Kumar Srivastava, J. Kumar, Effect of zinc addition and vacuum annealing time on the properties of spin-coated low-cost transparent conducting 1 at% Ga–ZnO thin films, Sci. Technol. Adv. Mater. 14 (2013) 065002 15pp.
[8] I. Winer, G.E. Shter, M. Mann-Lahav, G.S. Grader, Effect of solvents and stabilizers on sol–gel deposition of Ga-doped zinc oxide TCO films, J. Mater. Res. 26 (2011) 1309–1315.
[9] C. Muiva, T.S. Sathiaraj, K. Maabong, Chemical spray pyrolysis path to synthesis of ZnO microsausages from aggregation of elongated double tipped nanoparticles, Mater. Sci. Forum 706 (2012) 2577–2582.
[10] C.M. Muiva, T.S. Sathiaraj, K. Maabong, Effect of doping concentration on the properties of aluminium doped zinc oxide thin films prepared by spray pyrolysis for transparent electrode applications, Ceram. Int. 37 (2011) 555–560.
[11] A. Ashour, M.A. Kaid, N.Z. El-Sayed, A.A. Ibrahim, Physical properties of ZnO thin films deposited by spray pyrolysis technique, Appl. Surf. Sci. 252 (2006) 7844–7848.
[12] J.–H. Shin, D.–K. Shin, H.Y. Lee, J.–Y. Lee, Characteristics of gallium and aluminium co-doped ZnO (GAZO) transparent thin films deposited by using the PLD process, J. Korean Phys. Soc. 55 (2009) 947–951.
[13] K.M. Lin, P. Tsai, Parametric study on preparation and characterization of ZnO: Al films by sol–gel method for solar cells, Mater. Sci. Eng. B 139 (2007) 81–87.
[14] J.–H. Kang, M.–H. Lee, D.W. Kim, Y.S. Lim, W.–S. Seo, H.–J. Choi, The annealing effect on damp heat stability of AGZO thin films prepared by DC moving magnetron sputtering, Curr. Appl. Phys. 11 (2011) 333–336.
[15] J.H. Lee, Y.Y. Kim, H.K. Cho, J.Y. Lee, Microstructural characteristics and crystallographic evolutions of Ga-doped ZnO films grown on sapphire substrates at high temperatures by RF magnetron sputtering, J. Cryst. Growth 311 (2009) 4641–4646.
[16] N.A. Dahoudi, Comparative study of highly dense aluminium- and gallium-doped zinc oxide transparent conducting sol–gel thin films, Bull. Mater. Sci. 37 (2014) 1243–1248.
[17] V. Fathollahi, M.M. Amini, Sol–gel preparation of highly oriented gallium-doped zinc oxide thin films, Mater. Lett. 50 (2001) 235–239.
[18] F. Wu, L. Fang, Y.J. Pan, K. Zhou, L.P. Peng, Q.L. Huang, C.Y. Kong, Seebeck and magnetoresistive effects of Ga-doped ZnO thin films prepared by RF magnetron sputtering, Appl. Surf. Sci. 255 (2009) 8855–8859.
[19] W.S. Choi, E.J. Kim, S.G. Seong, Y.S. Kim, C. Park, S.H. Hahn, Optical and structural properties of ZnO/TiO_2/ZnO multi-layers prepared via electron beam evaporation, Vacuum 83 (2009) 878–882.
[20] T.P. Rao, M.C.S. Kumar, Resistivity stability of Ga doped ZnO thin films with heat treatment in air and oxygen atmospheres, J. Cryst. Process Technol. 2 (2012) 72–79.
[21] T.P. Rao, M.C.S. Kumar, Physical properties of Ga-doped ZnO thin films by spray pyrolysis, J. Alloy. Compd. 506 (2010) 788–793.
[22] B.J. Lokhande, M.D. Uplane, Structural, optical and electrical studies on spray deposited highly oriented ZnO films, Appl. Surf. Sci. 167 (2000) 243–246.
[23] A.R. Babar, P.R. Deshamukh, R.J. Deokate, D. Haranath, C.H. Bhosale, K. Y. Rajpure, Gallium doping in transparent conductive ZnO thin films prepared by chemical spray pyrolysis, J. Phys. D 41 (2008) 135404 6pp.
[24] R.S. Reddy, A. Sreedhar, A. Sivasankar Reddy, S. Uthanna, Effect of film thickness on the structural, morphological and optical properties of nanocrystalline ZnO films formed by RF magnetron sputtering, Adv. Mater. Lett. 3 (2012) 239–245.
[25] D.H. Zhang, T.L. Yang, J. Ma, Q.P. Wang, R.W. Gao, H.L. Ma, Preparation of transparent conducting ZnO:Al films on polymer substrates by r.f. magnetron sputtering, Appl. Surf. Sci. 158 (2000) 43–48.
[26] X.S. Wang, Z.C. Wu, J.F. Webb, Z.G. Liu, Ferroelectric and dielectric properties of Li-doped ZnO thin films prepared by pulsed laser deposition, Appl. Phys. A 77 (2003) 561–565.
[27] T.P. Rao, M.C.S. Kumar, Effect of thickness on structural, optical and electrical properties of nanostructured ZnO thin films by spray pyrolysis, Appl. Surf. Sci. 255 (2009) 4579–4584.
[28] M. Caglar, S. Ilican, Y. Caglar, F. Yakuphanoglu, Electrical conductivity and optical properties of ZnO nanostructured thin film, Appl. Surf. Sci. 255 (2009) 4491–4496.
[29] M. Mehrabian, R. Azimirad, K. Mirabbaszadeh, H. Afarideh, M. Davoudian, UV detecting properties of hydrothermal synthesized ZnO nanorods, Physica E 43 (2011) 1141–1145.
[30] M.C. Jun, S.U. Park, J.H. Koh, Comparative studies of Al-doped ZnO and Ga-doped ZnO transparent conducting oxide thin films, Nanoscale Res. Lett. 7 (2012) 639–645.
[31] Y.G. Wang, S.P. Lau, H.W. Lee, S.F. Yu, B.K. Tay, X.H. Zhang, K.Y. Tse, H.H. Hng, Comprehensive study of ZnO films prepared by filtered cathodic vacuum arc at room temperature, J. Appl. Phys. 94 (2003) 1597–1604.
[32] S.S. Shinde, P.S. Shinde, Y.W. Oh, D. Haranath, C.H. Bhosale, K.Y. Rajpure, Structural, optoelctronic, luminescence and thermal properties of Ga-doped zinc oxide thin films, Appl. Surf. Sci. 258 (2012) 9969–9976.
[33] R.A. Smith, Semiconductors, Academic Publishers, Calcutta 1989, pp. 461–463.
[34] C. Gümüş, O.M. Ozkendir, H. Kavak, Y. Ufuktepe, Structural and optical properties of zinc oxide thin films prepared by spray pyrolysis method, J. Optoelectron. Adv. Mater. 8 (2006) 299–303.
[35] M. Caglar, S. Ilican, Y. Caglar, Influence of dopant concentration on the optical properties of ZnO: in films by sol–gel method, Thin Solid Films 517 (2009) 5023–5028.
[36] P.K. Nayak, J. Yang, J. Kim, S. Chung, J. Jeong, C. Lee, Y. Hong, Spin-coated Ga-doped ZnO transparent conducting thin films for organic light-emitting diodes, J. Phys. D: Appl. Phys. 42 (2009) 035102.
[37] D.L. Zhang, J.B. Zhang, Q.M. Wu, X.S. Miao, Microstructure, morphology and ultraviolet emission of zinc oxide nanopolycrystalline films by the modified successive ionic layer adsorption and reaction method, J. Am. Ceram. Soc. 93 (2010) 3284–3290.
[38] F. Urbach, The long-wavelength edge of photographic sensitivity and of the electronic absorption of solids, Phys. Rev. 92 (1953) 1324.
[39] S.J. Ikhmayies, R.N. Ahmad-Bitar, A study of the optical bandgap energy and Urbach tail of spray-deposited CdS:In thin films, J. Mater. Res. Technol. 2 (2013) 221–227.
[40] K.L. Chopra, Thin Film Phenomena, MC Graw Hill, New York, USA 1969, p. 255.
[41] E. Reza, G.M. Reza, A. Hossein, Sol–gel derived Al and Ga co-doped ZnO thin films: an optoelectronic study, Appl. Surf. Sci. 290 (2014) 252–259.
[42] R.G. Gordon, Preparation and properties of transparent conductors, in: Proceedings of the Materials Research Society Symposium, Vol. 426, 1996, pp. 419–429.